Tidal modulation of incident wave heights: Fact or Fiction?

[1]M.A. Davidson, [1]T.J. O'Hare and [1]K.J. George

[1]School of Earth Ocean and Environmental Science,
University of Plymouth, Drake Circus, Plymouth, Devon, PL4 8AA, UK.
mdavidson@plymouth.ac.uk

ABSTRACT

This contribution investigates the hypothesis that incident wave power is modulated by the tide. Eulerian measurements of wave height recorded by three wave buoys in intermediate water depths (8-45 m A.C.D.), over a seven year period were analysed in a search for evidence of this semi-diurnal variability in incident wave heights. The study site (Perranporth, UK) was a highly macrotidal environment with a maximum spring tidal range of approximately 7.5 m. Autospectra of wave height time-series displayed a significant peak at semi-diurnal frequencies that was coherently coupled to the tidal displacement. At this site maximum wave power was seen to occur on the rising tide, on average 1 hour 6 minutes before high water. The observed semi-diurnal variability in wave height increases in magnitude towards the shoreline. This contribution presents field evidence for tidal modulation of incident wave power by the tide and suggests a possible explanation for the observations in terms of an analytical model for attenuation of wave power by contra tidal flows.

ADDITIONAL INDEX WORDS: *Wave-current interaction, viscous effects, tidal push, wave damping, wave dissipation*

INTRODUCTION

It has long been suggested by surfers (possibly the most avid group of wave-watchers) that in macro- tidal areas breaker heights commonly increase during the certain phases of the tide. Frequently, (but not exclusively) it is observed that incident wave height increases during the rising tide, a phenomenon is often referred to by surfers as the *'tidal push'*, The phrase 'tidal push' implies that the incoming tide somehow eases the passage of shoreward propagating waves, even providing them with extra energy, whilst the outgoing tide opposes the passage of waves, somehow dissipating wave energy. This pattern of wave height modification is at variance with conventional wave current interaction studies which show convincing evidence that wave heights will grow in adverse flows. Although observations of increasing wave height during the rising tide currently lack any solid scientific support they are extremely common and globally wide-spread amongst the surfing community. In the last two years the 'tidal push' phenomenon which is generally reported to follow a slack tide lull at low-tide has also received interest from the scientific community. This is evidenced by numerous communications documented on the coastal scientific communities' e-mail circular, the 'coastal list'. However, to the authors' knowledge there has currently been no data presented or formal publication to substantiate or reject these subjective observations. This contribution investigates the hypothesis that nearshore wave power can be modulated by the tide.

Tidal modulation of wave height not only impacts recreational surfers but also has serious ramifications in the area of nearshore sediment transport. Many engineering formulae and guidelines require only the input of wave statistics at breaking, these being derived from the predicted or measured offshore waves. Tidal asymmetry in wave patterns could lead to net sediment transport patterns that are not predicted by models which neglect this effect.

Clearly, in many cases there are very simple well documented explanations for the observation that incident wave heights vary coherently with the tidal level. In other cases the mechanisms are not at all clear. Some of the processes that could potentially contribute to wave height modulation at tidal frequencies are listed below:

1. **Refraction effects:** The combination of wave refraction and changing water levels due to tides can lead to semi-diurnal variability in the incident wave energy at specific coastal locations. This is a common observation both in sheltered embayments and in regions where the offshore bathymetry is complex (e.g. submarine canyons).
2. **Sea Breezes:** Sea breezes are known to enhance wave heights on a diurnal basis (MASSELINK, G. and PATTIARATCHI, 1998, 2001).
3. **Wave steepening by tidal flows:** Wave-current interaction may also potentially modulate incident wave heights (PEREGINE, D.H., 1976, HEDGES, 1987). Opposing tidal flows will lead to steepening of the incident wave field thus increasing the height of incident waves (although wave power is conserved).
4. **Wave dissipation by contra tidal flows:** It is possible that the wave steepening induced by opposing flows (3) will lead to enhanced dissipation (wave power is not conserved) which may ultimately result in a reduction in breaker height. The reverse will be true for following flows. Estimates of viscous damping of incident waves due to vertical shear in opposing currents has also been examined by THAIS *et al.,* (2001).
5. **Bottom friction:** Waves arriving at high tide propagate through deeper water thus experiencing less frictional dissipation due to shear stress at the sea floor (BATTJES AND JANSSEN, 1978; THORNTON and GUZA, BATTJES AND STIVE, 1985).
6. **Wave deflection by tidal flows:** Tidal flows deflect/refract incident waves as they propagate towards the coast.
7. **Wave reflection:** It is common for beaches to be increasingly reflective towards the high water mark. A consequence of this is that wave reflection generally increases towards high water (ELGAR *et al.*, 1994) sometimes leading to quasi-standing wave fields and localised enhancements in wave height.
8. **Complex morphological effects:** Similarly, a beach profile that becomes more reflective towards high water leads to a narrowing of the surfzone, a change in wave form from the spilling towards the plunging / surging extreme of the continuum and an enhanced rate of shoreward dissipation of wave energy. Furthermore, waves of a given height break in shallower water on a steeper foreshore (i.e. the break index increases) potentially giving rise to prolonged shoaling prior to breaking. These factors may combine to significantly modulate wave **breaker heights** at tidal frequencies even if incident wave power remains constant over the tidal cycle.

It is useful at this point to make a distinction between those processes that influence breaker heights by modulating the level of wave power incident to a given region of the surfzone (points 1-6) and those that will lead to modulations in breaker heights even if the incident wave power just prior to breaking is constant (Points 7-8). The challenge of elucidating which of these processes is responsible for the tidal push phenomenon is substantially complicated by the fact that several of these processes may be occurring simultaneously.

This paper is concerned only with the modulation of wave power prior to breaking and utilises data from wave buoy located seaward of the surfzone. First an analysis of field measurements of wave height recorded in a strongly macro-tidal environment is presented, looking for evidence of tidal modulations in wave power. Secondly, the nature of the tidal dynamics in the area where the observations were made is examined. Finally, possible explanations for the observations are made with the aid of a simple conceptual model.

STUDY AREA

Perranporth is located on the north coast of Cornwall on the southwest peninsula of the UK. Perranporth is an exposed section of the coast which is fully open to ocean swell with periods of 10-15 s, generated by the frequent depressions which generally track towards the study site from a westerly direction (Figure 1). The mean incident wave height for this area is about 1.5 m with waves frequently exceeding 5 m particularly during the winter season. Waves propagate from the North Atlantic over a shallow (<200m), broad (400km) continental shelf. Waves are predominantly normally incident to the beach with little refraction and minimal longshore currents.

The tidal regime is macrotidal with spring ranges of up to 7.5 m and offshore tidal flows reaching 1.2 m/s. Generally the dissipating effect of wave bottom friction in the shallow water close to the coast seems to reduce tidal flows close to the coast. Thus, tidal currents are generally low near the coast and in the surfzone.

The beach at Perranporth is a gently sloping (gradient = 0.02), dissipative beach (Wright and Short, 1984) with regular beach contours. The intertidal beach has a near linear slope with permanent offshore bar(s) located seawards of the low tide mark. The longshore variability in the coastal morphology is generally weak.

Field observations of incident wave height variability

In this section Eulerian measurements of wave height recorded in a strongly macrotidal environment are analysed in an attempt to find evidence for semi-diurnal variability in incident wave power. Data were recorded using four offshore wave rider buoys deployed near Perranporth beach. Measurements were made every three hours at 8.5 m, 13 m and 45 m water depth. Details of these wave measurements are summarised in Table 1 and the time series of wave height and synoptic tidal displacements are shown in Figure 2. Also included in Table 1 are data from the Seven Stones wave buoy which is located off the end of the south west peninsula in 60 m water depth (Figure 7).

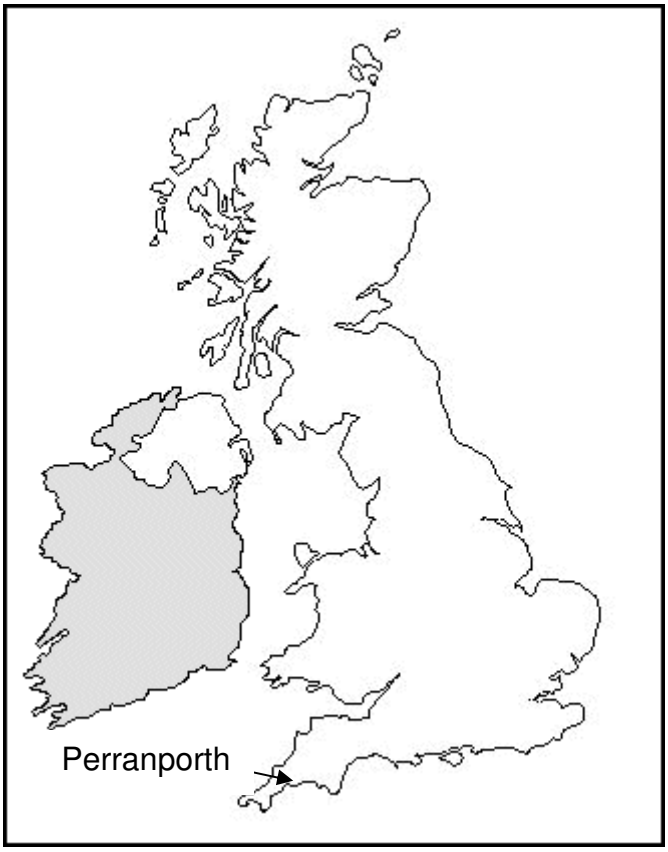

Figure 1. Location of the study site, Perranporth, Cornwall, UK.

Table 1. Wave data summary table. H_s = significant wave height, d = depth L_o = deep water wavelength

Lat. / Long.	Eastings/ Northings	Mean Depth d (m)	Period of data recording From	To	Duration (Years)	$\frac{\overline{H_s}}{H_{s,\max}}$ (m)	$\frac{d}{\overline{L_0}}$
Seven Stones 050°03.8'N 006°04.4'W	108531 26157	60	1/8/96	13/11/97	1.27	2.10 11.00	1.12 Deep
Perranporth 050°23'N 005°21'W	161878 59149	45	30/8/78	27/6/79	0.81	1.69 6.34	1.05 Deep
Perranporth 050°21.5'N 005°09.7'W	175144 55784	13	26/9/80	14/12/81	1.15	1.48 6.37	0.30 Int.
Perranporth 050°21'N 005°10.35'W	174334 54891	8.5	13/11/75	2/3/86	7.82	1.47 7.81	0.19 Int.

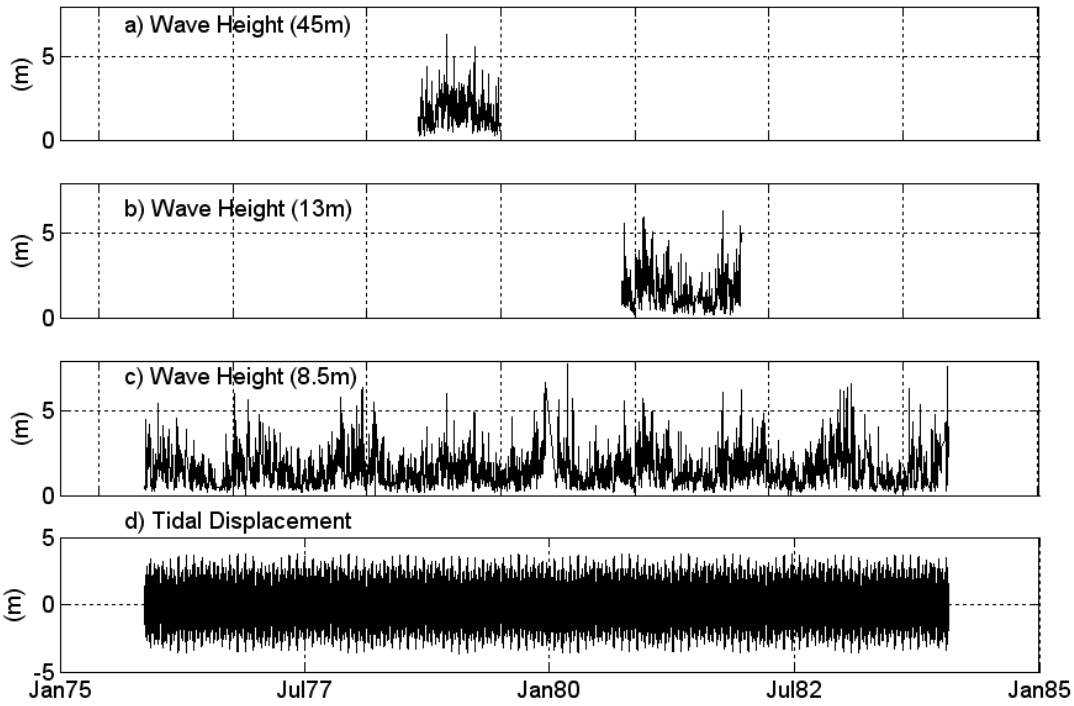

Figure 2. Time series of significant wave height collected at Perranporth in 8.5 m, 13 m and 45 m water depth together with the local predicted tidal displacement for Perranporth.

The highest variance in time series of wave height (Figure 2) occurs at seasonal frequencies with winter wave heights reaching over 6 m whilst summer wave heights seldom exceed 3 m. A spectral analysis of the longest of the three wave height time-series which was recorded in the shallowest region (8.5 m) is shown in Figure 3. The low-frequency portion of the spectrum clearly shows the peak at seasonal frequencies (0.0027 cycles/day). The mean magnitude of the seasonal signal (established by band-pass filtering the raw data with a frequency domain filter) is approximately 1.3 m. Of greater significance to the focus of this paper is the peak occurring at principal lunar semi-diurnal frequency (1.93 cycles/day) in the high frequency spectrum. This peak, although much smaller in magnitude than the seasonal peak is highly significant at the 99% confidence level and represents a modulation in the incident wave height at the wave recorder location of up to 40 cm (average values over 7.8 years = 14 cm) over a tidal cycle.

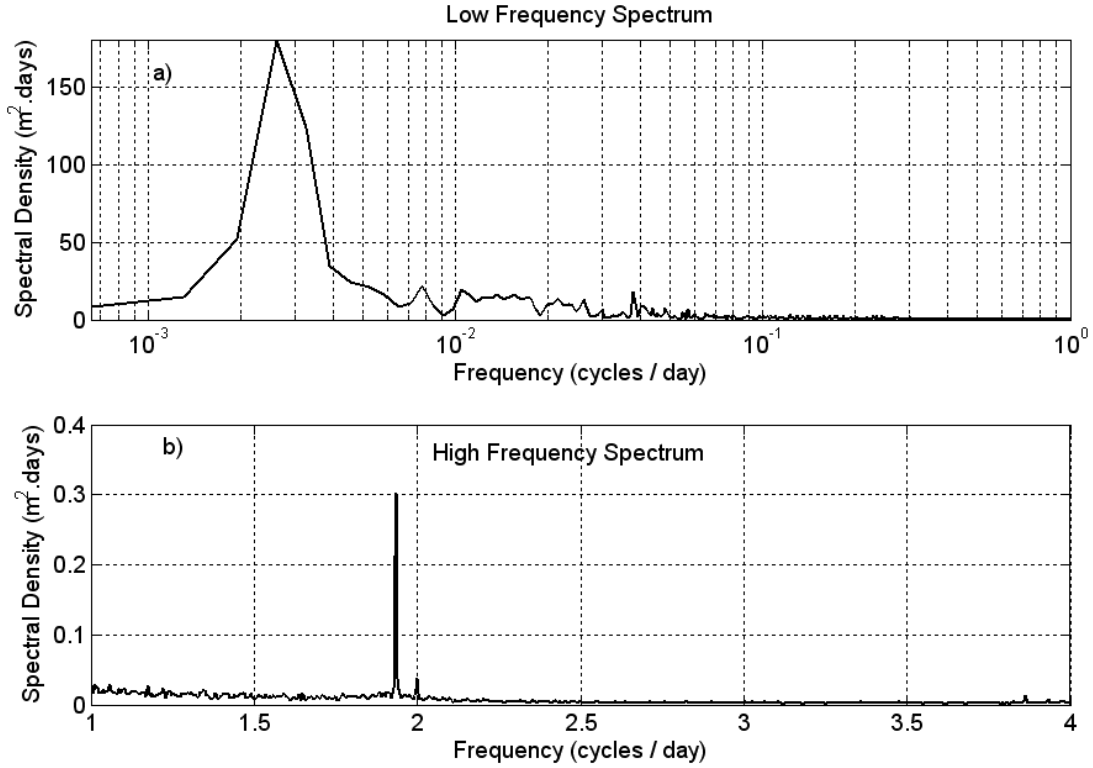

Figure 3. Low (a) and high (b) frequency spectra of the wave height time-series measure in 8.5 m of water. Note that the bandwidth of spectra 'a' and 'b' have been selected differently in order to exemplify the features of interest. The low frequency spectrum has a bandwidth of 6.51×10^{-4} cycles/day and shows a strong seasonal signal at 0.0027 cycles/day. The higher frequency spectrum has a bandwidth of 0.0039 cycles/day and displays a highly significant (at the 99% confidence level) semi-diurnal peak at 1.93 cycles/day.

A cross-spectral analysis of the wave height time series and tidal displacement is shown in Figure 4. The auto-spectrum of wave height (Figure 4a) and tidal elevation (Figure 4b) both show dominant peaks at semi-diurnal frequencies. These semi-diurnal peaks are highly coherent at the 95% confidence level (Figure 4c). Figure 4d shows the phase relationship between wave height time series and the tidal displacement for cross-spectral estimates having significant cross-coherence. Interestingly, the semidiurnal peak in wave height occurs on the rising phase of the tide (phase $\approx$-50 degrees) 1 hour 44 minutes before high tide. The confidence interval for the phase estimates corresponding to the semi-diurnal peak is ± 5 degrees so this can be estimated with some accuracy. Similarly, the errors in the phase of predicted tidal data are estimated to be less than 10 minutes.

Figure 5 investigates the variability in the semi-diurnal modulation in wave height with water depth and shows auto-spectra of the wave height time series at 8.5 m, 13 m, 45 m, (Perranporth) and 60 m (Seven Stones) water depth. Figure 5 show a progressive increase in the apparent tidal modulation with decreasing water depth. Whereas semidiurnal modulation in wave height time series were found to be completely absent at the Seven Stones wave buoy which is located in a depth of 60 m.

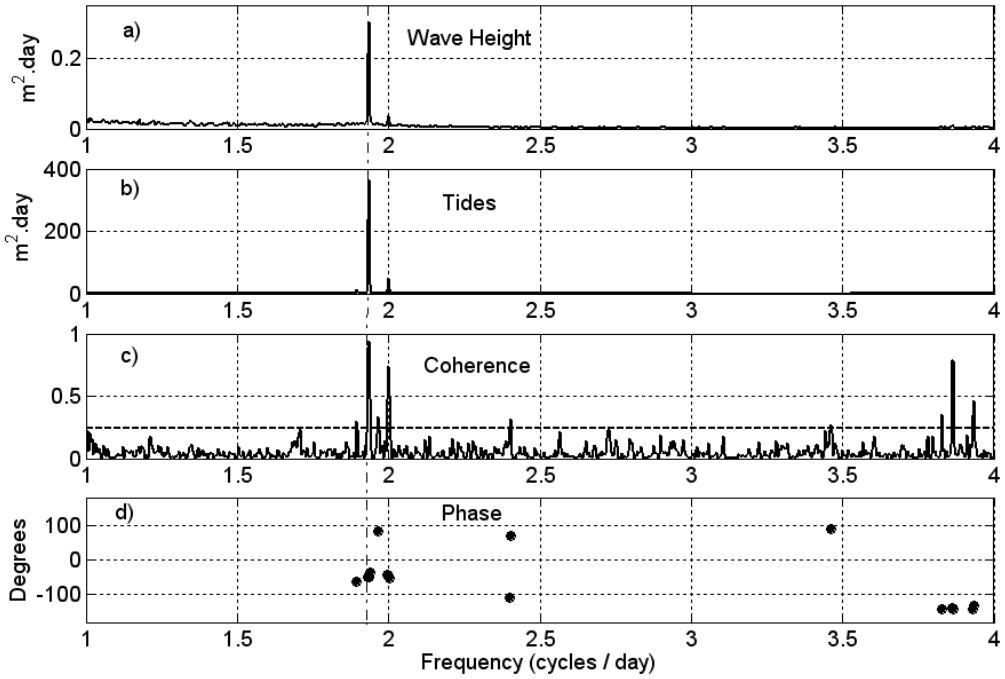

Figure 4. Cross-spectral analysis between wave height and tidal displacement time-series. a) Wave height spectral density function. b) Tides spectral density function. c) Cross-spectral coherence with 95% confidence interval (dotted horizontal line). d) Cross-spectral phase (plotted for coherent points only).

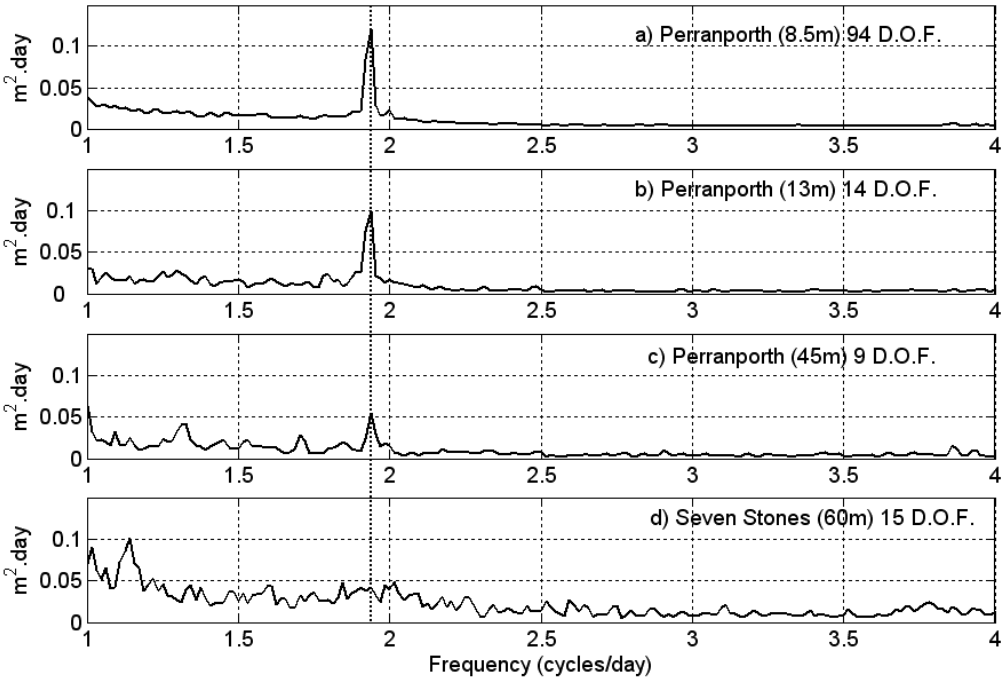

Figure 5. Spectra from 3 different stations at Perranporth in varying water depths (a-c) and in 60 m water depth at the Seven Stones wave recorder. All spectra have the same bandwidth (0.0156 cycles/day). The number of degrees of freedom (D.O.F.) of the spectral estimates differs in each case owing to the different record lengths.

The observed semi-diurnal variability in wave height measured at the shallower stations could be simply explained by the cross-shore variability in wave height $(\partial H/\partial x)$ caused by the wave shoaling pattern being advected passed the fixed wave recorder by the tidal displacement. Similar to the observations this effect would be expected to grow closer to the shore where $\partial H/\partial x$ is largest. However, in the absence of dissipation, wave power should remain approximately constant over the tidal period. Therefore the semidiurnal peak in the wave power spectrum should not be present in the absence of any true tidal modulation. This hypothesis is tested below using a simple linear wave theory approximation.

The incident wave power per unit area (Wm^{-2}) is given by:

$$P = cn\frac{1}{8}\rho g H^2 \tag{1}$$

Where ρ is the density of water, g is is the acceleration due to gravity, c is the wave celerity;

$$c = \frac{gT}{2\pi}\tanh(kd) \tag{2}$$

and,

$$n = \frac{1}{2}\left[1 + \frac{2kd}{\sinh(2kd)}\right] \tag{3}$$

Here T is the wave period and k is the wave number. Notice that the effects of refraction have not been considered here which is a reasonable assumption given that this site faces due west into the path of the prevailing Atlantic swell. Note also that the calculation of wave speed (equation 2) takes no account of the modifications due to following or contra tidal flows. Equation 1 was used to predict the wave power time series at the 8.5 m buoy station. The resulting cross-spectral analysis with the tidal data can be seen in Figure 6.

Interestingly the magnitude of the semi-diurnal spectral peak in the wave power spectrum remains highly significant at the 95% level, (Figure 6a) with high cross-spectral coherence between the tidal displacement, (Figure 6c). The cross-spectral phase at semi-diurnal frequency is approximately -32^{o}, which corresponds to a peak in incident wave power approximately 1 hour 6 minutes before high tide.

It is concluded from this analysis that the observed semidiurnal variance in the wave record is not completely due to simple wave shoaling. The regional tidal flow patterns are examined in the following section in order to determine possible wave current interaction effects.

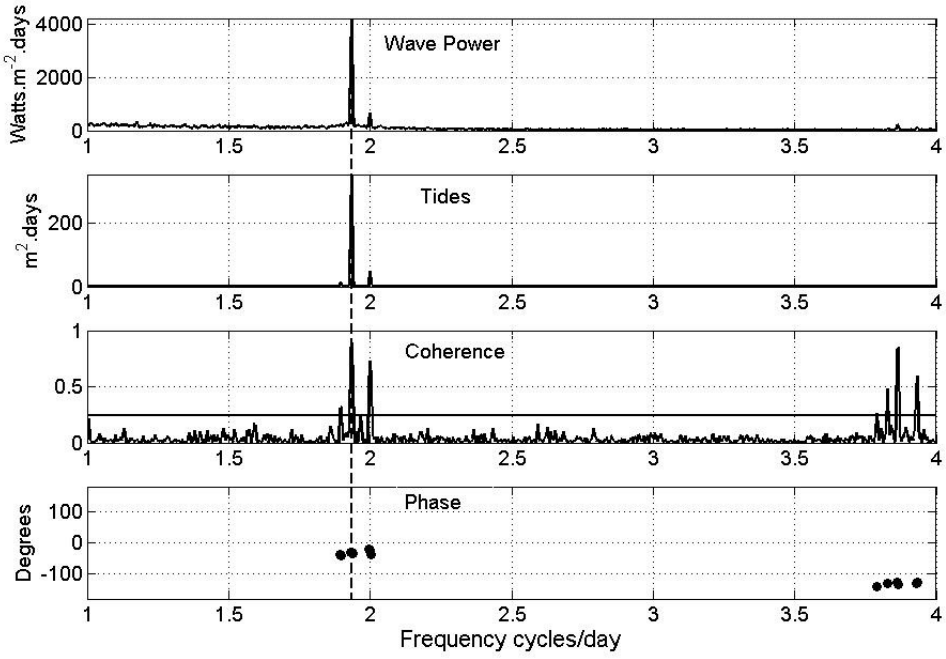

Figure 6. a) Measured wave power spectrum at 8m depth. b) Tidal elevation spectrum. c) Cross-spectral coherence. d) Coherent phase estimates, (bandwidth =0.0039 cycles/day)

TIDAL MODEL PREDICTIONS AT PERRANPORTH

The tidal stream atlas for mean spring tides was produced by running a 2D tidal numerical model using the VICTOR software (GEORGE, 2003). This software solves the depth-integrated equations of motion and continuity using a finite-difference technique. The model covers the coastal zone from Bideford Bay to Lyme Bay, including the Isles of Scilly. It uses a grid 0'.8 in latitude by 1'.2 in longitude, and uses as input on the open boundaries data from ROBINSON (1979) and from SINHA and PINGREE (1997).

Some example model output is shown in Figure 7 for selected intervals measured in solar hours relative to high water (HW) at Perranporth. In Figure 7 only a subset of the model grid points have been displayed to improve clarity. Off Perranporth, the northeast-going stream (here labelled flood) begins at approximately HW-5 hours (Figure 7a), reaching a maximum velocity just after HW-2 hours (Figure 7b) and continues to run until HW+1 hour (Figure 7c). It is interesting to note that the time of maximum flood just precedes the maximum wave power at Perranporth (observed at 1hour 6 minutes before HW) and that the component rate in the direction of wave propagation (west to east) is high (up to 0.7 m/s). Conversely, although tidal flows reach a similar magnitude at the Seven Stones Buoy they run predominantly north-south, i.e. perpendicular to the direction of wave propagation.

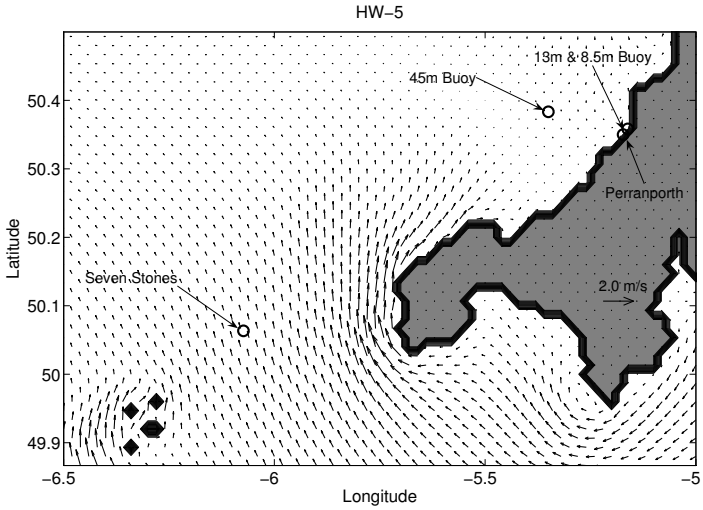

a)

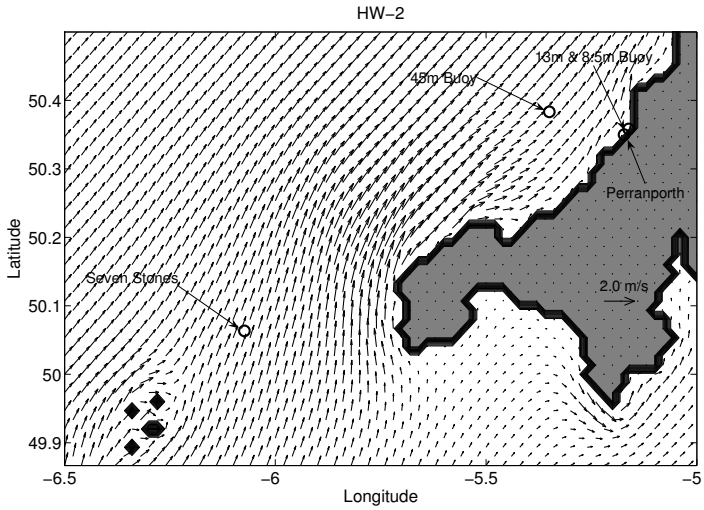

b)

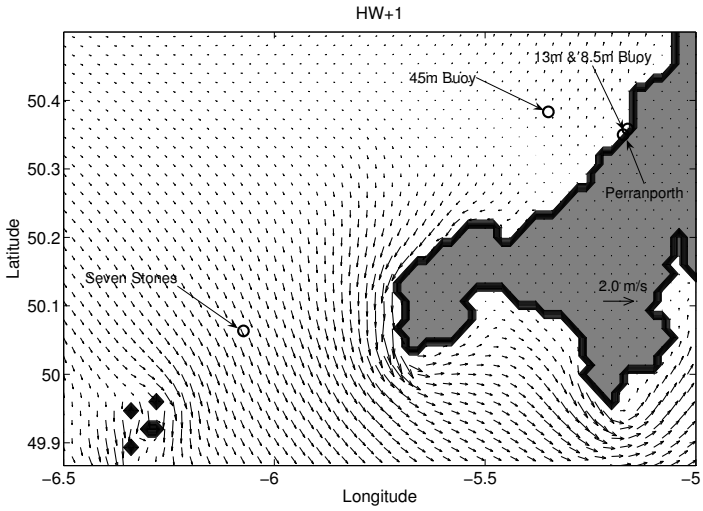

c)

Figure 7. Model prediction of tidal velocity vectors during the northeast-going (flood) stream. Note that the buoy locations are shown by the open circles.

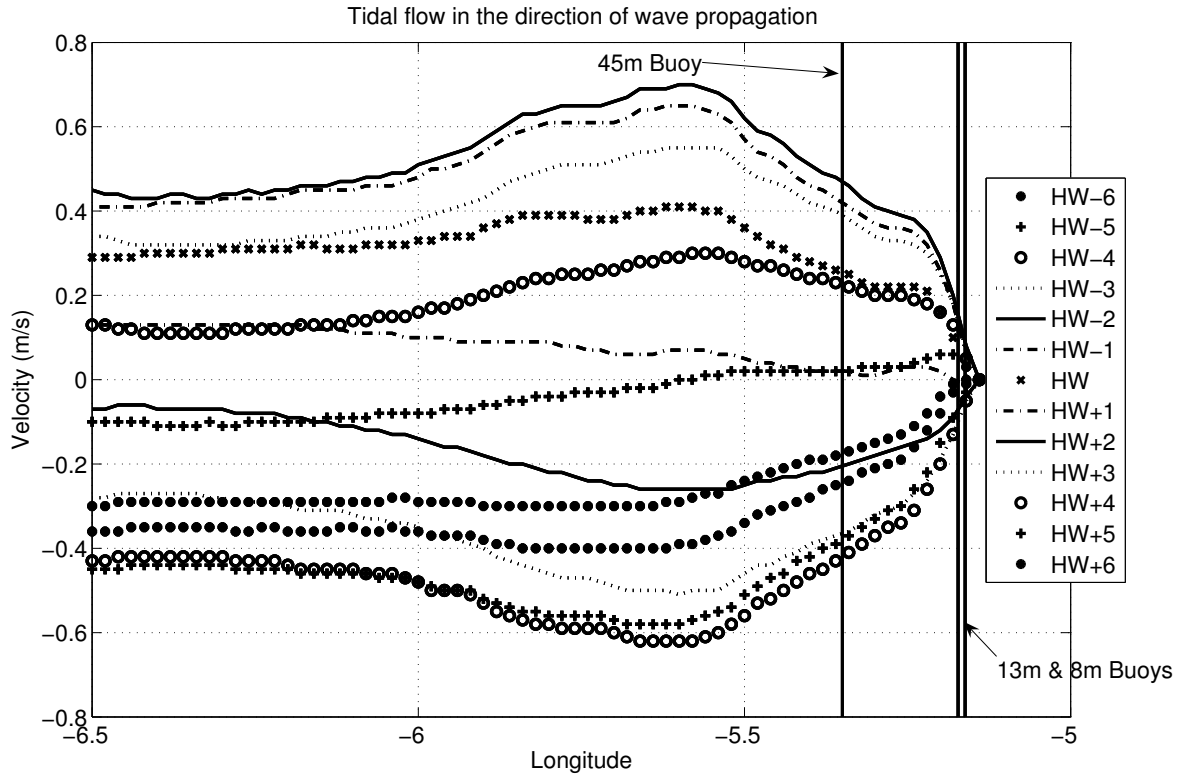

Figure 8. Spatial and temporal variations in tidal flow in the direction of wave propagation at latitude of 50°21'N (Perranporth). Note that the locations of the Perranporth wave buoys are shown by the vertical lines and the coast is located on the right hand side of the diagram where the current velocity vectors converge to zero.

The spatial and temporal variations of this component at latitude 50°21'N are shown in Figure 8. Directional wave measurements show that waves prevail from west to east, so only the easterly component of the tidal stream is considered in Figure 8. Tidal flows are seen to increase in magnitude in an eastward direction due to the effects of continuity in the shallower regions. The continuity effects are exceeded close to the coast by frictional dissipation leading to a rapid decay of tidal currents close to the coast. Indeed predicted tidal flows do not exceed about 0.1 m/s in the region of the shallowest buoys (8.5 m and 13 m) where the semidiurnal modulations are most prevalent. Further offshore at the 45 m station tidal flows can reach almost 0.5 m/s. Maximum resultant tidal flows in the wave propagation region are approximately 1.0 m/s.

Close inspection of the temporal variability in the tidal flows clearly shows that the maximum flows in the direction of wave propagation occur approximately two hours prior to high water across the whole domain at this latitude. Maximum flows which are contrary to the direction of wave propagation occur between four and five hours after high water.

A SIMPLE MODEL FOR WAVE DAMPING IN OPPOSING TIDAL FLOWS

In order to examine the possible influence of wave damping due to the propagation of waves through a time-varying (tidal) current a simple analytical model was produced. At the heart of this model is the assumption that when waves propagate against a current they undergo enhanced dissipation and when they travel with a following current the dissipation is reduced. The model makes no attempt to estimate the absolute magnitude of the wave damping but rather tries to predict the timing of the maximum tidal push relative to the time of the maximum local following tidal flows. The model is not explicit about the precise mechanism for wave damping although it is anticipated that this variation could result from wave steepening during opposing current flow leading to wave breaking (e.g. through white-capping) or, more likely, be the result of increased frictional loss from the waves as they travel through an opposing momentum flux. Thais et al. (2001) and KEMP and SIMONS (1983) examined the process of viscous damping of waves by boundary induced turbulence caused by shear in steady flows. They found that the waves propagating downstream are less damped, and waves propagating upstream significantly more damped, than a fluid at rest. If boundary layer induced turbulence is a major source of wave damping one might anticipate that the level of dissipation would be highly depth dependent.

The model assumes that the waves travel into a region ($x > 0$) in which the wave energy dissipation varies sinusoidally with the tidal frequency (T_0) such that at time t and location x the dissipation may be written as:

$$\varepsilon = \varepsilon_0 - (1 + \delta x)\Delta\varepsilon \cos\left(2\pi \frac{t}{T_0} + \phi\right) \quad (4)$$

In this expression ε_0 is the mean wave energy dissipation, $\Delta\varepsilon$ is the amplitude of the variation of wave energy dissipation due to the presence of the tidal flow at $x = 0$ and ϕ is a phase angle. The factor δ allows the possible influence of varying tidal flow strength across the region to be examined (if $\delta > 0$ the tidal current strength increases across the region in which the tidal flows influence the wave damping). The expression is written such that the minimum instantaneous wave damping occurs if the total phase ($2\pi t/T_0 + \phi$) is zero (maximum following current).

Using this expression it is possible to determine the total wave energy dissipation which the waves present at location x at time t have experienced as they have travelled through the region of tidal influence. The aim here is to predict the phase relationship between the maximum local (i.e. at any location x) following currents and the incidence of maximum (least damped) wave heights (the 'tidal push'). It is anticipated that this phase angle will increase with the size of the friction patch that the waves propagate through.

By writing the tidal period T_0 in terms of the speed (c_0) and wavelength (L_0) of the tidal motion (assuming that these are constant in the region $x > 0$) and the location of the waves (x) at time t is related to the speed of wave propagation (c) (also assumed constant) the expression becomes;

$$\varepsilon = \varepsilon_0 - (1 + \delta x)\Delta\varepsilon \cos(\alpha x + \phi) \quad (5)$$

where,

$$\alpha = \frac{2\pi c_0}{c L_0} \quad (6)$$

The total wave damping experienced by waves at a location X as they travel through the time-varying tidal current is thus:

$$\varepsilon_{TOT} = \int_0^X \varepsilon_0 dx - \Delta\varepsilon \int_0^X (1+\delta x)\cos(\alpha x + \phi)dx \quad (7)$$

This leads to an expression for ε_{TOT} that is a function only of the phase angle ϕ, namely:

$$\varepsilon_{TOT}(X) = \varepsilon_0 X + \Delta\varepsilon\left\{\frac{\sin\phi}{\alpha} - \frac{(1+\delta X)\sin(\alpha X+\phi)}{\alpha} - \frac{\delta\cos(\alpha X+\phi)}{\alpha^2} + \frac{\delta\cos\phi}{\alpha^2}\right\} \quad (8)$$

Values for ϕ which correspond to the maximum and minimum values of ε_{TOT} can be obtained by evaluating the function:

$$\frac{d\varepsilon_{TOT}}{d\phi} = 0 \quad (9)$$

Performing this analysis produces an expression for the phase angles for minimum and maximum wave damping at the location X as follows:

$$\tan\phi = \frac{\alpha(1+\delta X)\cos\alpha X - \delta\sin\alpha X - \alpha}{\alpha(1+\delta X)\sin\alpha X + \delta\cos\alpha X - \delta} \quad (10)$$

Figure 9 shows the total phase for the occurrence of minimum damping (associated with maximum wave height) for a series of relative wave speed values (c/c_0 = 0.2, 0.4, 0.6, 0.8). According to the model, the maximum tidal push occurs after the maximum flood (total phase = zero) depending on the horizontal extent of the tidally-varying friction patch (X/L_0) and the relative wave speed, but for relative fast wave propagation and a small friction patch the maximum tidal push is found shortly after maximum flood (near zero phase) in common with the observations at Perranporth.

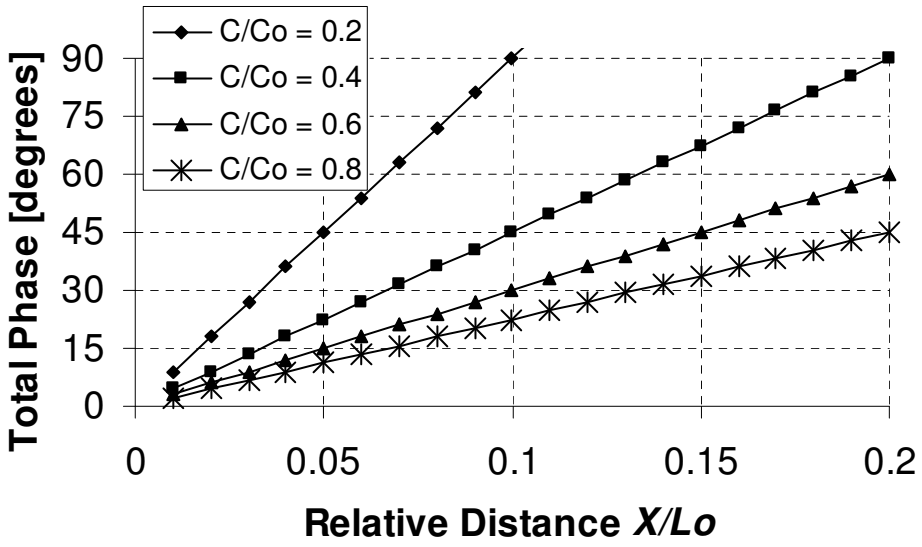

Figure 9: Total phase (measured relative to the time of maximum following tidal flows) for the occurrence of minimum damping (associated with maximum wave height) for a series of relative wave speed values.

DISCUSSION

The analysis of a 7.8 year wave height time-series has clearly demonstrated there is a significant semidiurnal variability in the wave power at this macrotidal location. These principal lunar frequency modulations are coherently linked to the tidal displacement with maximum wave power occurring at this site approximately 1 hour 6 minutes before high water. Furthermore it is noted from the tidal analysis conducted here that the time at which maximum wave power occurs slightly lags the time of the maximum following (flooding)

tidal streams. In this section the various mechanisms for wave height modulation at tidal frequencies are discussed in relation to the field observations at Perranporth. It is perhaps easiest to proceed by discussing each of the potential wave height modulation mechanisms (1-8 in the introduction) within the context of the measurements at Perranporth.

1. **Refraction effects:** Perranporth is an exposed beach which faces directly towards the North Atlantic. The beach is dissipative in nature with a beach gradient of approximately 0.02 and regular (parallel) seabed contours. The dominant direction of wave approach is approximately normal to the beach. Therefore wave refraction effects can be safely eliminated as a possible cause of wave height modulation at this site.

2. **Sea breeze effects:** Sea breezes are an infrequent occurrence at this site, but can be used to explain only diurnal and not semi-diurnal variability in incident wave heights; they are not thought to be of primary importance at this site.

3. **Wave steepening by tidal flows:** This mechanism does not provide a satisfactory explanation for the observations at this site although it is anticipated that tidal flows will significantly modify wave heights at the deepwater stations (the Seven Stones and 45 m depth buoys). The tidal analysis carried out in this paper indicates that wave steepening effects would be largest during the maximum ebb flow which occurs 4-5 hours after high water counter to observations. Furthermore, the tidal model predictions for this area suggests that close to the coast, damping of the tidal wave by seabed friction exceeds continuity effects leading to a reduction of tidal flows with decreasing water depths and consequently very low tidal currents (<0.1 m/s) in the region where the most significant semidiurnal variability was found. Moreover, since the observations show the tidal modulations in wave height increases shoreward this pattern does not fit the observations. However, it is anticipated that this mechanism will be important where tidal flows are rapid within the surf and breaker zones. Such anecdotal observations have been made around the United Kingdom in estuaries (e.g. North Sands Beach, Devon) and in the NE coast of Scotland (e.g. Fraserburgh, Grampion). In this situation wave heights are seen to increase during the falling tide contrary to the observations at Perranporth.

4. **Wave dissipation by contra tidal flows:** This contribution details a simple conceptual model for tidal damping in contra-tidal flows. The model is not specific about the mechanism for the damping but rather parameterises damping to be a minimum when tidal flows follow the direction of wave propagation and a maximum when opposing. The model predicts that the phase relationship between maximum following currents and maximum wave heights. Maximum following currents were measured at about 2 hours before high tide, whilst maximum wave power was measured on average 1 hour 6 minutes before high tide at Perranporth. The time of arrival of the maximum waves (which is predicted to be after the maximum currents) becomes progressively later the larger the distance the waves travel through the tidal flow field (i.e. the width of the friction patch). This distance is expressed as a relative distance in Figure 9 by dividing by the tidal wavelength (L_o). Furthermore, the phase is predicted to decrease as the propagation speed (cn) of the waves increased relative the speed of the tidal wave $\left(=\sqrt{gh}\right)$. At the edge of the continental shelf c/c_o is approximately 0.2 for wave with a period of 10 s. However, at depths of less than 100 m it increases rather rapidly reaching a value of 1 at the shoreline. Average values of c/c_o in the region of interest are approximately 0.6. The observed phase difference between the timing of maximum flows and wave heights at Perranporth can be estimated to be approximately 50-60 minutes. This is

equivalent to approximately 30 degrees of tidal phase. Taking these values the maximum width of the friction patch can be estimated at 0.1 in dimensionless units (X/L_o). Assuming a tidal wavelength of $O(10^6)$ m (a reasonable assumption for these depths) this is equivalent to a distance of approximately 100 km. This distance would encompass the peak in tidal flows offshore of the wave buoys shown in Figure 8. Thus, we may conclude that wave dissipation by contra tidal flows postulated here provides a feasible explanation for the timing of the maximum tidal push relative to the flood tidal streams and high-water.

5. **Bottom friction:** Dissipation of wave energy due to bottom friction can also be modelled with the simple model outlined in this contribution. The main difference is that instead of being phase coupled to the flows the damping mechanism is coupled with the surface elevation (like the wave shoaling effect), giving maximum and minimum damping following low and high tide respectively (counter to the observations at Perranporth). A further difference is that the effect of this frictional dissipation is topographically constrained to intermediate and shallow water depths rather than the region of significant tidal flows discussed previously. At Perranporth the area of intermediate and shallow water is relatively narrow (<13 km) compared to the region of significant tidal currents (>50km). Crude calculations using simple parameterisations for wave height attenuation due to bottom friction (BATTJES and JANSSEN, 1978; THORNTON and GUZA, 1983) indicate that the effect is likely to be almost imperceptible at Perranporth.

6. **Wave deflection by tidal flows:** The tidal analysis presented in this contribution shows that the strongest tidal flows are directed predominantly parallel to the direction of wave propagation (except at the Seven Stones location). It is unlikely therefore that the tangential components of the tidal flow are significant to deflect waves arriving through such a broad swell window away from the study site, although this cannot be fully tested without invoking a sophisticated wave-current interaction model.

7. **Wave reflection:** The low beach gradients and absence of any well developed bars above the low water line means that coastal reflection of gravity waves is likely to be extremely low at this study site, and therefore cannot explain the observed variability. Based on observations of reflection coefficients on natural beaches (ELGAR *et al*., 1994) it is anticipated that the reflection coefficient for surface gravity waves is likely to be less than 0.2.

8. **Complex morphological effects:** The variations in breaker heights induced by the changes in morpholology over a tidal cycle warrant further research but are not relevant to the observations here which were made seaward of the surfzone.

On balance therefore the observations seem to support the theory for wave dissipation in contra tidal flows. One curiosity however is the rather sudden increase in the semi-diurnal signal between the offshore location (45 m) and the inshore locations. These stations are separated by only 13 km so it is unlikely that the dissipation effects of opposing tidal flows will have such a large effect over this short range. The increase in semi-diurnal variability at the shallower station is only partially explained by the advection of the wave shoaling profile passed the fixed sensor array. It is likely that the larger waves arriving at the shallower station are reduced in amplitude at the offshore location (45 m depth) due to the inverse wave steepening effects produced following tidal flow. This flow is five times stronger at the 45 m station than at 8.5 m. Thus, in the deeper water where the tidal flows are strongest the wave steepening mechanism and dissipation due to contra tidal flows have an opposite effect, partially cancelling each other out. Semidiurnal modulation of wave heights at the Seven

Stones buoy is completely absent. It is hypothesised that this is due to the fact that the strongest tidal flows at this location are predominantly perpendicular to the direction of wave propagation.

CONCLUSIONS

1. Data recorded in a macrotidal environment shows clear evidence of tidal modulation of incident wave power at semi-diurnal frequencies.
2. At Perranporth (mean water depth = 8.5 m) the magnitude of the observed semidiurnal variability has maximum and mean annual values of 40 cm and 14 cm respectively.
3. The observed maximum in wave power consistently occurred consistently on the rising tide 1 hour 6 minutes prior to high tide.
4. The timing of maximum wave height occurs just after (50-60 minutes) the maximum flooding tidal currents which have a significant component of flow (0.7 m/s) in the direction of wave propagation.
5. The observed semi-diurnal modulations in incident wave height are not adequately explained at this site by:

- Wave refraction effects
- Wave shoaling effects
- Wave steepening in adverse flows (ignoring dissipation effects)
- See breezes
- Wave reflection
- Wave attenuation due to seabed friction
- Deflection of waves due to tangential flows
- Complex morphological affects

6. A simple model for wave dissipation due to opposing tidal flows provides qualitative support for the tidal damping of incident waves by contra-tidal flows.

REFERENCES

BATTJES, J.A. and JANSSEN, J.P.F.M. 1978. Energy loss and set-up due to breaking of random waves. Proc. 16th Conf. Coastal Eng., ASCE. 569-587.

BATTJES, J.A. and STIVE, M.J.F. 1985. Calibration and verification of a wave dissipation model for random breaking waves. J. Geophys. Res. **90**: 9159-9167.

ELGAR, S., HERBERS, T.H.C. and GUZA, R.T. 1994. J. Phys. Oceanography 24. 1503-1511.

GEORGE, K.J., 2003. VICTOR – a user's handbook. Internal report - University of Plymouth, School of Earth Ocean and Environmental Science, 12p.

HEDGES, T.S., 1987. Combinations of waves and currents: an introduction. Proc. Instn. Civ. Eng., Part 1, 82. 567-585.

KEMP, P.H. and SIMONS, R.R., 1983. The interaction between waves and turbulent current: waves propagating against the current. J. Fluid Mechanics, 130. 73-89.

MASSELINK, G. and PATTIARATCHI, C., 1998. C.B. Morphodynamic impact of sea breeze activity on a beach with beach cusp morphology. Journal of Coastal Research, **14(2)**, 393-406, ED 1061.

MASSELINK, G. and PATTIARATCHI C., 2001, C.B. Characteristics of the sea breeze system in Perth, Western Australia, and its effect on nearshore wave climate. Journal of Coastal Research , **17(1)**: 173-187, ED 1465.

PEREGRINE, D.H., 1976. Interaction of water waves and currents. Adv. Appl. Mech., **16**. 9-117.

ROBINSON, I.S., 1979. The tidal dynamics of the Irish and Celtic Seas. Royal Astronomical Society Geophysical Journal, 56(1), 159-197.

SINHA, B. and PINGREE, R.D. 1997, "The principal lunar semi-diurnal tide and its harmonics: baseline solutions for M2 and M4 constituents on the north-west European continental shelf." Cont. Shelf. Res., 17. 1321-1365.

THAIS, L. G. CHAPALAIN, G. KLOPMAN, R.R. SIMONS, and THOMAS G.P., 2001. Estimates of wave decay rates in the presence of turbulent currents. Applied Ocean Res. **23**: 125-137.

THORNTON, E.B. and R.T. GUZA, 1983. Transformation of wave height distribution. J. Geophys Res. **88**: 5925-5983.

WRIGHT, L.D. and SHORT A.D., 1983. Morphodynamics of beaches and surfzones in Australia. In CRC handbook of coastal processes and erosion, P.D. Komar (editor). 35-64. Boca Raton, FL: CRC Press.

ACKNOWLEDGEMENTS

The authors would like to thank Hydraulics Research Wallingford for the supply of the wave data used in this paper. We would like to thank the US Office of Naval Research NICOP programme for supporting research into long-term, large scale coastal behaviour. Finally, we would like to acknowledge Dr. Malcolm Findlay for sharing his experience of tidal modulation of wave height in areas that were unfamiliar to the authors putting a more global perspective on these observations.